Kinetic blockings in long-range interacting inhomogeneous systems

Jean-Baptiste Fouvry and Mathieu Roule
Institut d'Astrophysique de Paris, UMR 7095, 98 bis Boulevard Arago, F-75014 Paris, France

(Received 7 June 2023; accepted 11 October 2023; published 7 November 2023)

Long-range interacting systems unavoidably relax through Poisson shot noise fluctuations generated by their finite number of particles, N. When driven by two-body correlations, i.e., $1/N$ effects, this long-term evolution is described by the inhomogeneous $1/N$ Balescu-Lenard equation. Yet, in one-dimensional systems with a monotonic frequency profile and only subject to 1:1 resonances, this kinetic equation exactly vanishes: this is a first-order *full* kinetic blocking. These systems' long-term evolution is then driven by three-body correlations, i.e., $1/N^2$ effects. In the limit of dynamically hot systems, this is described by the inhomogeneous $1/N^2$ Landau equation. We numerically investigate the long-term evolution of systems for which this second kinetic equation also exactly vanishes: this a second-order *bare* kinetic blocking. We demonstrate that these systems relax through the "leaking" contributions of dressed three-body interactions that are neglected in the inhomogeneous $1/N^2$ Landau equation. Finally, we argue that these never-vanishing contributions prevent four-body correlations, i.e., $1/N^3$ effects, from ever being the main driver of relaxation.

DOI: 10.1103/PhysRevE.108.054108

I. INTRODUCTION

Following an initial violent relaxation happening on dynamical timescales [1], long-range interacting N-body systems end up on quasistationary states. Force fluctuations driven by finite-N shot noise then unavoidably lead to the long-term relaxation of these systems, driving them ever closer to their thermodynamical equilibrium. Fixing the system's total mass, the larger the number of particles N, the slower this relaxation. Kinetic theory aims at describing such long-term irreversible evolutions and spans a wide range of physical systems [2–5]. In the present paper, we are interested in inhomogeneous systems, i.e., integrable systems with a nontrivial mean-field orbital structure [3], as is the case, for example, in galactic discs [6], galactic nuclei [7], or globular clusters [8].

In self-gravitating systems, particles generate the potential within which they evolve. As such, any fluctuation in the particles' distribution is associated with a gravitational potential's perturbation. These self-consistent fluctuations are referred to as collective effects or equivalently as dressing (e.g., Debye shielding in plasmas [2]). Limiting oneself to two-body correlations, i.e., $1/N$ effects, the relaxation of self-gravitating systems is described by the inhomogeneous Balescu-Lenard (BL) equation [9,10]. In systems with weak pairwise interactions, i.e., in the dynamically hot limit, collective effects may be neglected. Then, the BL equation reduces to the inhomogeneous Landau equation [11]. When operating, the Landau equation describes a relaxation happening on a timescale of order $T_{\rm d}N/G^2$, with $T_{\rm d}$ the dynamical time and G the amplitude of the pairwise interaction potential.

Yet, in inhomogeneous 1D systems with a monotonic frequency profile and only subject to 1:1 resonances, both the Landau and BL collision operators exactly vanish, whatever the considered mean distribution function (DF) for the system. This is a kinetic blocking [12–18]. Such a situation cannot typically occur in higher dimensions, where nontrivial and nonlocal resonances prevent the $1/N$ collision operator from exactly canceling. While undergoing a kinetic blocking, systems can only evolve under the weaker contributions of three-body correlations, i.e., through $1/N^2$ effects. In the limit where collective effects can be neglected (i.e., the dynamically hot limit), Ref. [19] derived an inhomogeneous self-consistent closed kinetic equation describing this relaxation which occurs on a timescale of order $T_{\rm d}N^2/G^4$. We refer to this equation as the inhomogeneous $1/N^2$ Landau equation.

Interestingly, Ref. [19] pointed out the existence of a class of interaction potentials for which the inhomogeneous $1/N^2$ Landau equation also exactly vanishes—whatever the considered mean DF. We call this a second-order *bare* kinetic blocking, where *bare* emphasizes here that this blocking only holds in the limit where collective effects are neglected. In the present paper, we are interested in the long-term evolution of such peculiar systems. Placing ourselves in the dynamically hot limit, we show that their relaxation occurs, in fact, on a (slower) timescale of order $T_{\rm d}N^2/G^6$. We detail how such a scaling stems from a "leakage" of collective effects. We also argue that even when undergoing a second-order bare kinetic blocking, these systems' relaxation is still dominated by $1/N^2$ effects and not by four-body correlations, i.e., $1/N^3$ effects. Consequently, we claim that the (still unknown) inhomogeneous $1/N^2$ BL equation cannot vanish and that its contribution always dominates over contributions from four-body correlations.

The paper is organized as follows. In Sec. II, we detail our system. In Sec. III, we recall the kinetic equations at play and explain the various kinetic blockings. In Sec. IV, we investigate numerically the long-term relaxation of the considered system. We conclude in Sec. V. Throughout the main text, technical details are kept to a minimum and deferred to Appendices or to relevant references.

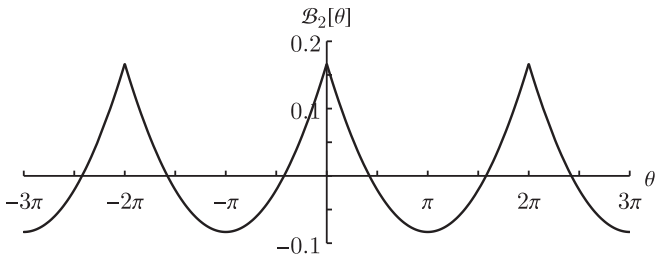

FIG. 1. Angular dependence, $\mathcal{B}_2(\theta)$, from the interaction potential of Eq. (2).

II. THE SYSTEM

Let us consider a set of N particles of individual mass $\mu = M_{\rm tot}/N$ with $M_{\rm tot}$ the system's (fixed) total mass. We denote the 1D canonical (specific) phase space coordinates $\mathbf{w} = (\theta, J)$, with θ the 2π-periodic angle and J the associated action [3]. We consider a total specific Hamiltonian given by

$$H_{\rm tot} = \sum_{i=1}^{N} U_{\rm ext}(\mathbf{w}_i) + \sum_{i<j}^{N} \mu\, U(\mathbf{w}_i, \mathbf{w}_j), \tag{1}$$

with $U_{\rm ext}(\mathbf{w})$ some given external potential and $U(\mathbf{w}, \mathbf{w}')$ some pairwise interaction potential, whose typical amplitude is denoted G. In practice, we assume the symmetry $U(\mathbf{w}, \mathbf{w}') = U(|\theta - \theta'|, \{J, J'\})$. This system is said to be inhomogeneous because the pairwise interaction does depend on the particles' actions. This choice also ensures usual conservation laws [see Eq. (E2)]. In addition, the pairwise interaction can be Fourier expanded as $U(\mathbf{w}, \mathbf{w}') = \sum_{k,k'} \delta_k^{k'} U_k(J, J') \mathrm{e}^{\mathrm{i}k(\theta-\theta')}$. Here, the Kronecker symbol, $\delta_k^{k'}$, imposes $k = k'$, which we refer to as the system only sustaining 1:1 resonances.

The system's statistics is described via the DF, $F = F(\mathbf{w}, t)$, normalized to $\int \mathrm{d}\mathbf{w} F = M_{\rm tot}$. Here and throughout, the range of integration is fixed to $\int \mathrm{d}\mathbf{w} = \int_0^{2\pi} \mathrm{d}\theta \int_{-\infty}^{+\infty} \mathrm{d}J$, where, importantly, the action coordinate is assumed to have an infinite support [20]. We also assume that the mean DF, $F = F(J, t)$, only depends on the action and time t. Similarly, the mean Hamiltonian, $H(\mathbf{w}) = U_{\rm ext}(\mathbf{w}) + \int \mathrm{d}\mathbf{w}' U(\mathbf{w}, \mathbf{w}') F(\mathbf{w}')$, is assumed to satisfy $H = H(J)$. From it, we can define the mean orbital frequencies $\Omega(J) = \mathrm{d}H/\mathrm{d}J$. Finally, since both the mean DF and mean Hamiltonian only depend on the action coordinates, Jeans theorem [22] ensures the quasistationarity of its mean-field dynamics.

For the rest of this paper, we will focus on one particular interaction potential, namely, Eq. (D6) of Ref. [19]. This interaction potential allows one to design kinetically blocked systems as we will detail in Sec. III. It reads [39]

$$U(\mathbf{w}, \mathbf{w}') = G\,(J - J')^2\, \mathcal{B}_2[\theta - \theta'], \tag{2}$$

with $\mathcal{B}_2(\theta) = B_2[\frac{1}{2\pi} w_{2\pi}(\theta)]$, $B_2(x) = x^2 - x + \frac{1}{6}$ the second Bernoulli polynomial, and the angle wrapping function

$$0 \leqslant w_{2\pi}(\theta) < 2\pi; \quad w_{2\pi}(\theta) \equiv \theta\ [2\pi]. \tag{3}$$

The function $\mathcal{B}_2(\theta)$ is illustrated in Fig. 1. We note that $\int \mathrm{d}\theta \mathcal{B}_2[\theta] = 0$, so $F(J)$ never generates any mean potential. Mean-field quantities such as the frequency profile are therefore fully determined by the external potential $U_{\rm ext}(\mathbf{w})$.

In this paper, we investigate the long-term evolution of systems driven by Eq. (2) in the dynamically hot limit. In that context, it corresponds to the limit $G \ll G_{\rm crit}$ (abusively denoted $G \to 0$), where $G_{\rm crit}$ stands for the critical value of G above which the system becomes linearly unstable (see Appendix A).

To highlight various regimes of relaxation, we explore three different external potentials, i.e., three different frequency profiles. More precisely, fixing the prefactors to unity, we consider

Frequency profiles

$$(1) \quad \Omega(J) = |J|, \tag{4a}$$

$$(2) \quad \Omega(J) = J\,|J|, \tag{4b}$$

$$(3) \quad \Omega(J) = J. \tag{4c}$$

And, for each case, we will consider the same initial DF, $F(J) \propto \exp(-J^4)$, which does not correspond to the thermal equilibrium of any of these profiles.

III. KINETIC BLOCKINGS

Given some interaction and external potentials, kinetic theory aims at predicting $\partial F(J,t)/\partial t$, i.e., the rate of orbital redistribution, in the statistical limit $N \gg 1$. Let us now sketch the equations describing the evolution of the previous systems at successive orders in $1/N$, highlighting, in particular, how kinetic blockings may occur.

A. First-order kinetic equation

Accounting only for two-body correlations, assuming linear stability, and neglecting collective effects, the system's relaxation is described by the inhomogeneous Landau equation [11]. Limiting ourselves to 1:1 resonances, it reads

$$\frac{\partial F(J)}{\partial t} \propto \mu \frac{\partial}{\partial J} \Bigg[\sum_{k_1} k_1 \int \mathrm{d}J_1\, |U_{k_1}(\mathbf{J})|^2 \times \delta_{\rm D}(\mathbf{k}\cdot\mathbf{\Omega})\, \mathbf{k}\cdot\frac{\partial}{\partial \mathbf{J}} F_2(\mathbf{J}) \Bigg], \tag{5}$$

where the time dependence was omitted for clarity (see Appendix B for the full expression). We recall that $\mu = M_{\rm tot}/N$, i.e., this relaxation is driven by $1/N$ effects. In Eq. (5), we shortened the notations using the two-vectors $\mathbf{J} = (J, J_1)$, $\mathbf{\Omega} = (\Omega[J], \Omega[J_1])$ and $\mathbf{k} = (k_1, -k_1)$, and $F_2(\mathbf{J}) = F(J)F(J_1)$. This equation also involves the bare coupling coefficients, $U_{k_1}(\mathbf{J})$, namely, the Fourier transform in angles of the pairwise interaction potential (see Appendix B). When taking collective effects into account, Eq. (5) becomes the inhomogeneous BL equation [9,10]. It follows from Eq. (5) with the substitution $|U_{k_1}(\mathbf{J})|^2 \to |U_{k_1}^{\rm d}[F](\mathbf{J})|^2$, with the dressed coupling coefficients $U_{k_1}^{\rm d}[F](\mathbf{J})$ detailed in Appendix B.

On long timescales, two particles can efficiently couple to one another and drive relaxation only if they share commensurate orbital frequencies. This is visible in Eq. (5) through the presence of the Dirac delta, $\delta_{\rm D}(\mathbf{k}\cdot\mathbf{\Omega})$. For a system with a monotonic frequency profile, $J \mapsto \Omega(J)$, the resonance condition $\delta_{\rm D}(\mathbf{k}\cdot\mathbf{\Omega})$ imposes $J_1 = J$ (a so-called local resonance), so the cross term, $\mathbf{k}\cdot\partial F_2/\partial\mathbf{J}$, in Eq. (5) exactly vanishes. Ultimately, this leads to $\partial F(J)/\partial t = 0$, i.e., the kinetic equation predicts no relaxation. Importantly, for a monotonic frequency profile, we stress that this cancellation holds (i) whatever the considered interaction potential, $U(\mathbf{w},\mathbf{w}')$; (ii) whatever the considered (stable) DF, $F(J)$; and (iii) for both the Landau and BL equations, i.e., independently of whether collective effects are or are not accounted for. This is a first-order *full* kinetic blocking: such systems cannot relax via two-body correlations ($1/N$ effects). In that case, the relaxation is greatly delayed and can only occur through three-body correlations ($1/N^2$ effects).

B. Second-order kinetic equation

Placing themselves within this regime and neglecting collective effects, Ref. [19] derived a closed kinetic equation describing relaxation driven by $1/N^2$ effects. This inhomogeneous $1/N^2$ Landau equation is of the form

$$\frac{\partial F(J)}{\partial t} \propto \mu^2 \frac{\partial}{\partial J}\Bigg[\sum_{k_1,k_2}(k_1+k_2)\int \mathrm{d}J_1\mathrm{d}J_2\,|\Lambda_{k_1k_2}(\mathbf{J})|^2 \times \delta_{\rm D}(\mathbf{k}\cdot\mathbf{\Omega})\,\mathbf{k}\cdot\frac{\partial}{\partial\mathbf{J}}F_3(\mathbf{J})\Bigg], \tag{6}$$

and we refer to Appendix C for the full expression of the equation and the coupling coefficients, $|\Lambda_{k_1k_2}(\mathbf{J})|^2$. In Eq. (6), notations are shortened using here the three-vectors $\mathbf{J} = (J, J_1, J_2)$, $\mathbf{\Omega} = (\Omega[J], \Omega[J_1], \Omega[J_2])$ and $\mathbf{k} = (k_1+k_2, -k_1, -k_2)$, and $F_3(\mathbf{J}) = F(J)F(J_1)F(J_2)$. Since collective effects have been neglected, it is crucial to note that the coupling coefficients, $|\Lambda_{k_1k_2}(\mathbf{J})|^2$, only depend on the pairwise interaction potential: they do *not* involve the system's DF, $F(J)$. In Eq. (6), the resonance condition on orbital frequencies, $\delta_{\rm D}(\mathbf{k}\cdot\mathbf{\Omega})$, becomes more intricate than the one in Eq. (5). Indeed, it now involves three particles with commensurate orbital frequencies. This allows for nonlocal resonances, i.e., triplet of actions, $\mathbf{J}$, which are not all identical.

The generalization of Eq. (6) to account for collective effects, i.e. the inhomogeneous $1/N^2$ BL equation, is currently unknown. In particular, at order $1/N^2$, one may expect collective effects to be more involved than a simple dressing of the pairwise interaction potential see, e.g., footnote 5 in Ref. [23]. Nonetheless, in Eq. (6), we note that the cross term, $\mathbf{k}\cdot\partial F_3/\partial\mathbf{J}$, does not explicitly involve the interaction potential and its precise form is key to ensure all the conservation laws and H theorem of the kinetic equation [19]. As a consequence, we expect that the inhomogeneous $1/N^2$ BL equation can be obtained from Eq. (6) through some intricate substitution $|\Lambda_{k_1k_2}(\mathbf{J})|^2 \to |\Lambda^{\rm d}_{k_1k_2}[F](\mathbf{J})|^2$, which is still unknown.

In Eq. (6), the three-body cross term, $\mathbf{k}\cdot\partial F_3/\partial\mathbf{J}$, never vanishes at resonance except for the thermodynamical equilibrium (see Sec. IV.C in Ref. [19]). In that sense, three-body collisions always involve nontrivial resonances and cannot generically vanish whatever the DF: this is in sharp contrast with the first-order kinetic blocking of Eq. (5).

The goal of further delaying the relaxation described by Eq. (6), was investigated in Sec. IV.D of Ref. [19]. Therein, they showed that the pairwise potential from Eq. (2) in conjunction with profile (3) from Eq. (4c) ensures that $\Lambda_{k_1k_2}(\mathbf{J}) = 0$ at resonance. Phrased differently, the vanishing condition obtained in Ref. [19] amounted to devising $\Omega(J)$ and $U(\mathbf{w},\mathbf{w}')$ so that $\delta_{\rm D}(\mathbf{k}\cdot\mathbf{\Omega})\,\Lambda_{k_1k_2}(\mathbf{J}) = 0$. In that case, one gets $\partial F(J)/\partial t = 0$ in Eq. (6), i.e., this kinetic equation predicts no relaxation whatever the considered (stable) $F(J)$. We call this a second-order *bare* kinetic blocking.

Let us emphasize that the first-order blocking of Eq. (5) relies on the vanishing of the crossed term $\mathbf{k}\cdot\partial F_2/\mathbf{J} = 0$ at resonance, while the second-order blocking of Eq. (6) relies on the vanishing of the coupling coefficients $\Lambda_{k_1k_2}(\mathbf{J}) = 0$ at resonance. This is a fundamental difference. Indeed, the vanishing of the bare coefficients, $\Lambda_{k_1k_2}(\mathbf{J})$, does not imply the vanishing of the dressed coefficients, $\Lambda^{\rm d}_{k_1k_2}[F](\mathbf{J})$, because dressing depends on the considered DF. Since $\Lambda^{\rm d}_{k_1k_2}[F](\mathbf{J})$ will generically be nonzero at resonance, the inhomogeneous $1/N^2$ BL equation is not expected to vanish. We claim that this prevents any system from ever undergoing a second-order *full* kinetic blocking.

C. Scalings of the relaxation

Let us now detail the scaling of the relaxation time with respect to the total number of particles N and the amplitude of the pairwise interaction, G, in these various regimes.

In Eqs. (5) and (6), the scaling with respect to N is straightforwardly read from the dependence with respect to the individual mass $\mu = M_{\rm tot}/N$. One has $\partial F/\partial t \propto 1/N$ (respectively, $\propto 1/N^2$) in Eq. (5) [respectively, Eq. (6)]. In the present dynamically hot limit, the scaling with respect to G stems from the scaling of the coupling coefficients. In Eq. (5), one has $U_k \propto G$, so $\partial F/\partial t \propto G^2$. As for Eq. (6), the bare coupling coefficients, $\Lambda(\mathbf{J})$, are quadratic in the interaction potential, i.e., $\Lambda(\mathbf{J}) \propto G^2$ (see Appendix C). As a consequence, Eq. (6) leads to $\partial F/\partial t \propto G^4$. To summarize, in the dynamically hot limit, the $1/N$ Landau Eq. (5) predicts a relaxation timescale of order $T_{\rm r} \propto T_{\rm d}N/G^2$. And, in the same hot limit, the $1/N^2$ Landau Eq. (6) predicts a relaxation on the (slower) timescale $T_{\rm r} \propto T_{\rm d}N^2/G^4$. In both cases, the larger the number of particles, the slower the evolution; the stronger the interaction, the faster the evolution.

Now, we need to consider the case of systems subject to a second-order bare kinetic blocking. In the dynamically hot limit, i.e., for $G \to 0$, one expects for the $1/N^2$ dressed coefficients, $\Lambda^{\rm d}[F](\mathbf{J})$, to converge to the bare ones, $\Lambda(\mathbf{J})$. Since $\Lambda(\mathbf{J}) \propto G^2$, this leads to an expansion of the form

$$\Lambda^{\rm d}[F](\mathbf{J}) \underset{G\to 0}{=} \Lambda(\mathbf{J}) + G^3\Lambda^{\rm d}_{(3)}[F](\mathbf{J}) + O(G^4). \tag{7}$$

For systems undergoing a second-order bare kinetic blocking, one has $\Lambda(\mathbf{J}) = 0$ at resonance. As a consequence, in the hot limit, one finds the asymptotic scaling $\Lambda^{\rm d}[F](\mathbf{J}) \propto G^3$.

Given that $\partial F/\partial t \propto |\Lambda^{\rm d}[F](\mathbf{J})|^2$, systems subject to a second-order bare kinetic blocking are therefore expected to relax on a timescale of order $T_{\rm r} \propto T_{\rm d} N^2/G^6$. In that limit, relaxation is driven by leaks from dressed three-body interactions. Phrased differently, $1/N^2$ effects, albeit made less efficient by a second-order bare kinetic blocking, are always driving some nonzero relaxation in the present long-range interacting inhomogeneous 1D systems. We claim that one cannot design a system in which three-body correlations would systematically drive no dynamics, whatever the considered DF.

One could be worried that four-body correlations, i.e., $1/N^3$ effects, could drive relaxation more efficiently than the previous leaks from three-body collective effects. In Appendix D, placing ourselves in the hot limit, we justify that $1/N^3$ effects drive relaxation on a timescale of order $T_{\rm r} \propto T_{\rm d}\, N^3/G^6$, i.e., a subdominant process. As a conclusion, even if it was derived, an inhomogeneous $1/N^3$ Landau equation can never be the main driver of relaxation in the asymptotic limit $N \gg 1$. This is one of the main results of the present paper.

IV. NUMERICAL MEASUREMENTS

Let us now recap for each of the frequency profiles considered in Eqs. (4) the scaling of the relaxation time expected as one varies the total number of particles, N, and the amplitude of the pairwise coupling, G. We recall that we place ourselves within the limit of a dynamically hot system, i.e., $G \to 0$.

(1) Profile (1). This profile is nonmonotonic. This allows for nonlocal resonances, $J_1 \neq J$, in the $1/N$ Landau Eq. (5). The system is not subject to any kinetic blocking. We then expect $T_{\rm r} \propto T_{\rm d} N/G^2$.

(2) Profile (2). This profile is monotonic, so the $1/N$ Landau and BL operators both vanish. The $1/N$ dynamics is *fully* blocked. The system can only relax through $1/N^2$ effects, as governed by Eq. (6) in the hot regime. Profile (2) is not submitted to any second-order bare kinetic blocking, i.e., Eq. (6) gives a nonvanishing contribution. We expect then the scaling $T_{\rm r} \propto T_{\rm d} N^2/G^4$.

(3) Profile (3). This profile is monotonic, hence the $1/N$ dynamics is fully blocked. In addition, following Ref. [19], this profile is also submitted to a second-order bare kinetic blocking, i.e., the $1/N^2$ Eq. (6) vanishes. Yet, even though the $1/N^2$ Landau equation is zero whatever the considered DF, we argued in Sec. III C that leaks from the (yet unknown) $1/N^2$ BL equation will lead to a relaxation time scaling like $T_{\rm r} \propto T_{\rm d} N^2/G^6$ and not like $T_{\rm r} \propto T_{\rm d} N^3/G^6$ as one could have (wrongly) guessed from the four-body correlations contribution (see Appendix D).

To summarize, the profiles from Eqs. (4) are predicted to be associated with relaxation times scaling like

Relaxation times

$$(1)\quad T_{\rm r} \propto T_{\rm d} N/G^2, \tag{8a}$$

$$(2)\quad T_{\rm r} \propto T_{\rm d} N^2/G^4, \tag{8b}$$

$$(3)\quad T_{\rm r} \propto T_{\rm d} N^2/G^6. \tag{8c}$$

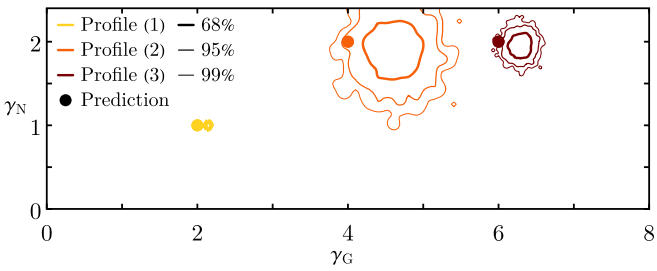

FIG. 2. Dependence of the relaxation time, via the power-law indices (γ_N, γ_G) from Eq. (9), as a function of the total number of particles, N, and the strength of the pairwise interaction, G, for the various frequency profiles from Eqs. (4) (associated with different colors). Points correspond to the kinetic predictions from Eqs. (8), while contours are obtained from N-body measurements (see Appendix E). A contour labeled $x\%$ contains $x\%$ of the measured power indices: the thinner the contour, the larger the fraction of measurements it encompasses (see Appendix E 6). As explained in Appendix E 7, a systematic bias towards higher γ_G is to be expected.

We set out to recover numerically the scalings predicted in Eqs. (8). To do so, for a given frequency profile, we explore a 5×5 grid of values of (N, G) running for each a large batch of 10^3 simulations. We then estimate from these the dependence of the relaxation time with respect to (N, G). We refer to Appendix E for details on how dynamics driven by Eq. (2) may be efficiently integrated.

In practice, we search for a power-law dependence of the form

$$T_{\rm r} \propto T_{\rm d}\, N^{\gamma_N}/G^{\gamma_G}, \tag{9}$$

and constraints on the power indices (γ_N, γ_G). A handful of reasons make these measurements challenging.

First, one needs to ensure that G is small enough for collective effects to be negligible, though large enough so that relaxation can still be observed numerically. We rely on linear response theory (Appendix A) to determine appropriate ranges in G.

Second, long-time integrations of the model from Eq. (2) are challenging, given the limited smoothness of this interaction potential. To ease this exploration, we accelerate the evaluation of the forces using an (exact) multipole method, as detailed in Appendix E 2. We also carefully pick our integration parameters to keep the global integration errors under control (Appendix E 4).

Finally, since we consider simulations with a small number of particles, the estimation of the relaxation time requires some care to prevent possible biases (Appendix E 6).

In Fig. 2, we report our main result, namely, the measurement of the power indices (γ_N, γ_G) from Eq. (9) as one varies the considered frequency profile.

In that figure, we first recover that all profiles exhibit their expected scaling with respect to N, i.e., the value of γ_N. In particular, even though profile (3) is submitted to a second-order bare kinetic blocking, i.e., Eq. (6) exactly vanishes, its relaxation is still driven by $1/N^2$ effects, i.e., three-body correlations. Once again, we emphasize that this particularly slow relaxation is sourced by leaks from dressed three-body correlations and not by four-body correlations.

In Fig. 2, we also find that all profiles show scalings with respect to G, i.e., the value of γ_G, in agreement with the predictions, though one could be suspicious about the systematic bias in the value of γ_G, which is always measured to be larger than the predicted one. We argue that this was to be expected since the measurements were made for a finite value of G, while the predictions correspond to the limit $G \to 0$. In particular, given the difficulty of integrating the motion driven by the potential from Eq. (2) (see Appendix E 3), we had to limit ourselves to considering not so dynamically hot systems (see Table I). In Appendix E 7, we show that the bias observed in Fig. 2 is well within the limits that could be expected from the effective use of finite values of G.

Ultimately, Fig. 2 allows us to numerically confirm the scaling of the relaxation times predicted in Eqs. (8), along with all the signatures associated with these various kinetic blockings.

V. CONCLUSIONS

In this paper, we investigated the long-term evolution of long-range interacting inhomogeneous 1D systems. In particular, we highlighted the existence of two types of kinetic blockings: (i) a first-order *full* kinetic blocking in systems with a monotonic frequency profile and only subject to 1:1 resonances, associated with the vanishing of the inhomogeneous $1/N$ BL equation; and (ii) a second-order *bare* kinetic blocking associated with the vanishing of the inhomogeneous $1/N^2$ Landau equation.

Considering a fixed interaction potential [Eq. (2)], we presented a large numerical exploration to confirm the existence of these various blockings. In particular, we showed that dynamically hot systems submitted to a second-order bare kinetic blocking still relax via $1/N^2$ effects, as a result of leaks from collective effects. We argued that the (still unknown) $1/N^2$ BL collision operator would never vanish as the cancellation of the $1/N^2$ Landau operator arises from very specific conditions on the coupling terms, which change when taking collective effects into account. Hence, four-body correlations, i.e., $1/N^3$ effects, can never be the main driver of the relaxation of long-range interacting inhomogeneous systems, even in the present contrived 1D geometry. As such, no system will ever suffer from a second-order *full* kinetic blocking, and we claim that the $1/N^3$ Landau equation does not need further investigation.

The present numerical work is only one more step towards a finer understanding of (very) long-term dynamics and high-order correlations. Naturally, it would be worthwhile and rewarding to derive the $1/N^2$ BL equation, hence generalizing Eq. (6). This is no easy task, and we feel that a realistic road map would be to perform such a delicate calculation first for the (single-harmonic) homogeneous Hamiltonian mean-field model [24,25], then for homogeneous systems with an arbitrary potential of interaction [26], and ultimately for the present inhomogeneous regime. Ultimately, this line of work would convincingly show that second-order kinetic blockings can never lead to the full vanishing of $1/N^2$ effects.

In the present paper, the action coordinate is assumed to have an infinite support. This is not generically true for inhomogeneous systems, where the action domain may be semi-infinite or even finite. For such setups, it has been shown that the presence of a minimum/maximum action drastically slows down the decay of perturbations, which only vanish algebraically with time [27–30]. It would then be worthwhile to investigate how such a finite or semi-infinite range of actions and the associated long-lasting perturbations affect the present kinetic blockings. We reserve this to future works.

Finally, we also assumed that the system remains linearly stable throughout its whole evolution. However, there exist cases for which the system's global thermodynamical equilibrium is magnetized, i.e., its DF, $F = F_{\rm eq}(\theta, J)$, has a nontrivial angular dependence [43] (see, e.g., Refs. [16,17,31,32]). In that case, although the kinetically blocked DF, $F = F(J, t)$, initially evolves slowly on a timescale of order $N^2 T_{\rm d}$, it unavoidably becomes linearly unstable at some point. This triggers a dynamical phase transition, and the DF (rapidly) "magnetizes" to become $F = F(\theta, J, t)$. The relaxation toward the thermodynamical equilibrium, $F_{\rm eq}(\theta, J)$, then keeps proceeding. Yet, this dynamics does not suffer from a first-order kinetic blocking because nonlocal resonances are now permitted. As a result, in this second stage of evolution, the relaxation occurs on a timescale of order $NT_{\rm d}$. Therefore, the overall dependence with respect to N of the total relaxation time toward the thermodynamical equilibrium must exhibit an intermediate scaling between N and N^2. Interestingly, this agrees with the scaling $N^{3/2}$ reported in Fig. 6 of Ref. [32] which considered long-range coupled classical spins. Naturally, in the light of the present kinetic theories, it would be informative to further investigate the impact on relaxation of such dynamical phase transitions, a question closely related to marginal stability crossing (see, e.g., Refs. [33,34]).

ACKNOWLEDGMENTS

This work is partially supported by Grant No. Segal ANR-19-CE31-0017 of the French Agence Nationale de la Recherche and by Idex Sorbonne Université. We warmly thank S. Rouberol for the smooth running of the Infinity cluster where the simulations were performed. We warmly thank C. Pichon for stimulating discussions.

APPENDIX A: LINEAR RESPONSE THEORY

In this Appendix, we rely on linear response theory (see, e.g., Sec. 5.3 in Ref. [3]) to estimate a system's dynamical temperature. This allows us to then carefully pick the value of G to place ourselves within the dynamically hot limit. Because the interaction potential from Eq. (2) is neither fully attractive nor repulsive, we first need to (slightly) generalize the computation of the response matrix compared to the typical gravitational case.

1. Basis elements

Let us consider a unidimensional Hamiltonian system with the angle-action coordinates $\mathbf{w} = (\theta, J)$. Taking inspiration from Ref. [35], we define a set of potential/density basis

elements $(\psi^{(p)}, \rho^{(p)})$ via

$$\psi^{(p)}(\mathbf{w}) = \int \mathrm{d}\mathbf{w}'\, \rho^{(p)}(\mathbf{w}')\, U(\mathbf{w}, \mathbf{w}'), \quad \text{(A1a)}$$

$$\int \mathrm{d}\mathbf{w}\, \rho^{(p)}(\mathbf{w})\, \psi^{(q)*}(\mathbf{w}') = -\gamma_p\, \delta_p^q, \quad \text{(A1b)}$$

where $\gamma_p = \pm 1$. With such a convention, the case $\gamma_p = +1$ (respectively, -1) corresponds, typically, to the attractive case (respectively, repulsive). Using Eqs. (A1), one can decompose the interaction potential as

$$U(\mathbf{w}, \mathbf{w}') = -\sum_p \psi^{(p)}(\mathbf{w})\, \Gamma_{pq}\, \psi^{(q)*}(\mathbf{w}'), \quad \text{(A2)}$$

with the diagonal matrix $\Gamma_{pq} = \gamma_p \delta_p^q$. The usual self-gravitating case corresponds to $\mathbf{\Gamma} = \mathbf{I}$, the identity matrix.

2. Response matrix

Following Kalnajs's matrix method [35] and paying particular attention to the basis normalization (see, e.g., Ref. [36]), the susceptibility of the self-gravitating system is captured by the dielectric matrix

$$\mathbf{E}(\omega) = \mathbf{\Gamma} - \mathbf{M}(\omega), \quad \text{(A3)}$$

with the response matrix

$$M_{pq}(\omega) = -2\pi \sum_k \int_{\mathcal{L}} \mathrm{d}J\, \frac{k\, \partial F/\partial J}{k\, \Omega(J) - \omega}\, \psi_k^{(p)*}(J)\, \psi_k^{(q)}(J). \quad \text{(A4)}$$

In this expression, we used the Fourier transform of the basis elements given by

$$\psi_k^{(p)}(J) = \int \frac{\mathrm{d}\theta}{2\pi}\, \psi^{(p)}(\mathbf{w})\, \mathrm{e}^{-\mathrm{i}k\theta}. \quad \text{(A5)}$$

We refer to Ref. [37] and references therein for a discussion on the resonant denominator, $1/(k\Omega(J) - \omega)$, and the associated Landau integral, $\int_{\mathcal{L}} \mathrm{d}J$.

We stress that the response matrix scales as $\mathbf{M}(\omega) \propto G$ since the potential basis elements (and therefore their Fourier transform) scale like $\psi^{(p)} \propto \sqrt{G}$. Consequently, in the dynamically hot limit, i.e., $G \to 0$, one has $\mathbf{E}(\omega) \to \mathbf{\Gamma}$. The smaller G, the smaller the collective effects.

3. Natural basis elements

We now focus on the interaction potential from Eq. (2). We aim at constructing natural basis elements for it, following Eqs. (A1). Equation (2) can be rewritten as

$$\begin{aligned} U(\mathbf{w}, \mathbf{w}') &= G\, (J - J')^2\, \mathcal{B}_2[\theta - \theta'] \\ &= G\, U_J(J, J')\, U_\theta(\theta, \theta'). \end{aligned} \quad \text{(A6)}$$

We decompose the angular part of the potential with

$$\begin{aligned} U_\theta(\theta, \theta') &= \mathcal{B}_2[\theta - \theta_2] \\ &= \frac{1}{\pi^2} \sum_{k=1}^{+\infty} \frac{1}{k^2} \cos[k(\theta - \theta')] \\ &= \sum_{p_\theta \neq 0} \frac{1}{2\pi^2} \frac{1}{p_\theta^2}\, \mathrm{e}^{\mathrm{i}p_\theta \theta}\, \mathrm{e}^{-\mathrm{i}p_\theta \theta'}. \end{aligned} \quad \text{(A7)}$$

Following an approach similar to Sec. A2 in [38], we periodise the function $U(J, J')$ on a period $2J_L$. More precisely, we define $U_{\mathrm{per}}(J, J') = U(J, J')$ for $|J - J'| \leqslant J_L$ and $U_{\mathrm{per}}(J + 2kJ_L, J') = U_{\mathrm{per}}(J, J')$ for $k \in \mathbb{Z}$. Then, we have the Fourier decomposition

$$\begin{aligned} U_{\mathrm{per}}(J, J') &= \frac{1}{3} J_L^2 + \sum_{p_J=1}^{+\infty} \frac{4(-1)^{p_J}}{\pi^2 p_J^2} J_L^2 \cos\left[p_J \frac{\pi}{J_L}(J - J')\right] \\ &= \frac{1}{3} J_L^2 + \sum_{p_J \neq 0} \frac{2(-1)^{p_J}}{\pi^2 p_J^2} J_L^2 \mathrm{e}^{\mathrm{i}p_J \frac{\pi}{J_L} J}\, \mathrm{e}^{-\mathrm{i}p_J \frac{\pi}{J_L} J'}. \end{aligned} \quad \text{(A8)}$$

We are now set to define our basis elements. We index them with $p = (p_\theta, p_J)$ (with $p_\theta \neq 0$), and introduce

$$\psi^{(p)}(\mathbf{w}) = \sqrt{|G|}\, a_\theta(p_\theta)\, a_J(p_J)\, \mathrm{e}^{\mathrm{i}p_\theta \theta}\, \mathrm{e}^{\mathrm{i}p_J \frac{\pi}{J_L} J}. \quad \text{(A9)}$$

In that expression, the (positive) coefficients $a_\theta(p_\theta)$ and $a_J(p_J)$ follow from Eqs. (A7) and (A8) and read

$$a_\theta(p_\theta) = 1/(\sqrt{2}\, \pi\, |p_\theta|), \quad \text{(A10)}$$

as well as

$$a_J(p_J) = \begin{cases} J_L/\sqrt{3} & \text{if } p_J = 0, \\ \sqrt{2} J_L/(\pi\, |p_J|) & \text{otherwise.} \end{cases} \quad \text{(A11)}$$

Following the convention from Eqs. (A1) (and reducing the action integration range to $-J_L \leqslant J \leqslant J_L$), one finds that the associated density elements read

$$\rho^{(p)}(\mathbf{w}) = \frac{(-1)^{p_J}}{4\pi J_L}\, \frac{\mathrm{Sign}[G]}{\sqrt{|G|}}\, \frac{\mathrm{e}^{\mathrm{i}p_\theta \theta}\, \mathrm{e}^{\mathrm{i}p_J \frac{\pi}{J_L} J}}{a_\theta(p_\theta)\, a_J(p_J)}. \quad \text{(A12)}$$

Finally, one finds the normalization constant

$$\gamma_p = -(-1)^{p_J}\, \mathrm{Sign}[G]. \quad \text{(A13)}$$

4. Computing the response matrix

Using the basis elements from Eq. (A9), whose Fourier transform satisfies $\psi_k^{(p)} \propto \delta_k^{p_\theta}$, we rewrite the response matrix from Eq. (A4) as

$$M_{pq}(\omega) = \delta_{p_\theta}^{q_\theta}\, A \int_{\mathcal{L}} \mathrm{d}J\, \frac{g(J)}{h(J) - \omega}, \quad \text{(A14)}$$

with

$$A = -2\pi\, |G|\, a_\theta^2(p_\theta)\, a_J(p_J)\, a_J(q_J) p_\theta, \quad \text{(A15a)}$$

$$g(J) = \frac{\partial F}{\partial J}\, \mathrm{e}^{-\mathrm{i}(p_J - q_J)\frac{\pi}{J_L} J}, \quad \text{(A15b)}$$

$$h(J) = p_\theta\, \Omega(J). \quad \text{(A15c)}$$

To carry out the integral in Eq. (A14), we truncate the domain $-J_L \leqslant J \leqslant J_L$ into K_J uniform intervals of length $\Delta J = 2J_L/K_J$ centred around the locations $J_k = -J_L + (k + \frac{1}{2})\Delta J$. Equation (A14) becomes

$$M_{pq}(\omega) = \delta_{p_\theta}^{q_\theta}\, A \sum_{k=1}^{K_J} I_k(\omega), \quad \text{(A16)}$$

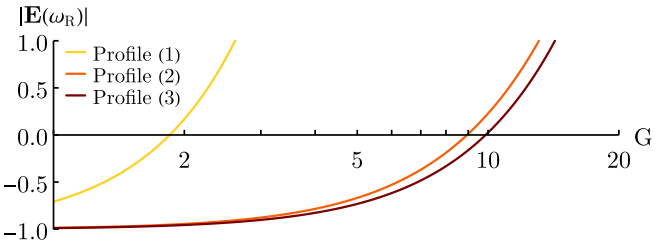

FIG. 3. Determinant of the dielectric matrix, $|\mathbf{E}(\omega_{\mathrm{R}}^{\mathrm{crit}})|$, as a function of G, for the profiles from Eqs. (4). For profile (1) [respectively, (2); (3)], the critical frequency is $\omega_{\mathrm{R}}^{\mathrm{crit}} \simeq 1.047$ [respectively, 0; 0]. The value of G_{crit} is reached when $|\mathbf{E}(\omega_{\mathrm{R}}^{\mathrm{crit}})|$ crosses zero.

with the integrals

$$I_k(\omega) = \int_{\mathcal{L}}^{J_k+\Delta J/2} \mathrm{d}J \, \frac{g(J)}{h(J)-\omega} \simeq \int_{\mathcal{L}}^{\Delta J/2} \mathrm{d}\delta J \, \frac{g_0 + g_1 \delta J}{h_0 + h_1 \delta J - \omega}, \tag{A17}$$

using a first-order expansion with $g_0 = g(J_k)$, $g_1 = g'(J_k)$, and a similar notation for (h_0, h_1).

The final step of the calculation is to compute

$$I_k(\omega) \simeq \int_{\mathcal{L}}^{1} \mathrm{d}u \, \frac{\bar{g}_0 + \bar{g}_1 u}{u - \varpi}, \tag{A18}$$

with $\bar{g}_0 = g_0/|h_1|$, $\bar{g}_1 = g_1 \Delta J/(2h_1)$ and the rescaled frequency $\varpi = 2(\omega - h_0)/(|h_1|\Delta J)$. We recall that the resonant denominator in that expression has to be interpreted using Landau's prescription (see, e.g., Ref. [3]). In practice, we use the expression presented in Sec. D of Ref. [37], evaluated for purely real frequencies. The computation presented in Appendix A 5 used $J_L = 5$, $K_J = 10^4$, $p_\theta = 1$, and $|p_J| \leqslant 100$.

5. Nyquist contours

Owing to the Kronecker symbol $\delta_{p_\theta}^{q_\theta}$ in Eq. (A14), $\mathbf{E}(\omega)$, as defined in Eq. (A3), is diagonal with respect to the angular index p_θ, so the p_θ can be considered independently of one another. Moreover, since $a_\theta[p_\theta] \propto 1/|p_\theta|$ [Eq. (A10)], the largest values of the response matrix are obtained for $p_\theta = \pm 1$. Finally, by symmetry, we may limit ourselves to $p_\theta = 1$ when assessing the system's linear stability.

For a given profile, we define the critical coupling amplitude, G_{crit}, as

$$G_{\mathrm{crit}} = \mathrm{Min}\{\, G > 0 \,|\, \exists\, \omega_{\mathrm{R}} \in \mathbb{R} \;\; \text{s.t.} \;\; |\mathbf{E}(\omega_{\mathrm{R}})| = 0\}, \tag{A19}$$

with $|\mathbf{E}(\omega)|$ the complex determinant. Systems with $0 \leqslant G < G_{\mathrm{crit}}$ are linearly stable. And, the smaller G/G_{crit}, the hotter the system and the more negligible collective effects are. In Fig. 3, we represent the dependence of $G \mapsto |\mathbf{E}(\omega_{\mathrm{R}}^{\mathrm{crit}})|$, where the (real) frequency, $\omega_{\mathrm{R}}^{\mathrm{crit}}$, is the frequency of the system's first oscillating mode. It satisfies $\mathrm{Im}[|\mathbf{E}(\omega_{\mathrm{R}}^{\mathrm{crit}})|] = 0$ for all G as well as $|\mathbf{E}(\omega_{\mathrm{R}}^{\mathrm{crit}})| = 0$ for $G = G_{\mathrm{crit}}$. From that figure, we readily determine the values of G_{crit} for each profile, as reported in Table I.

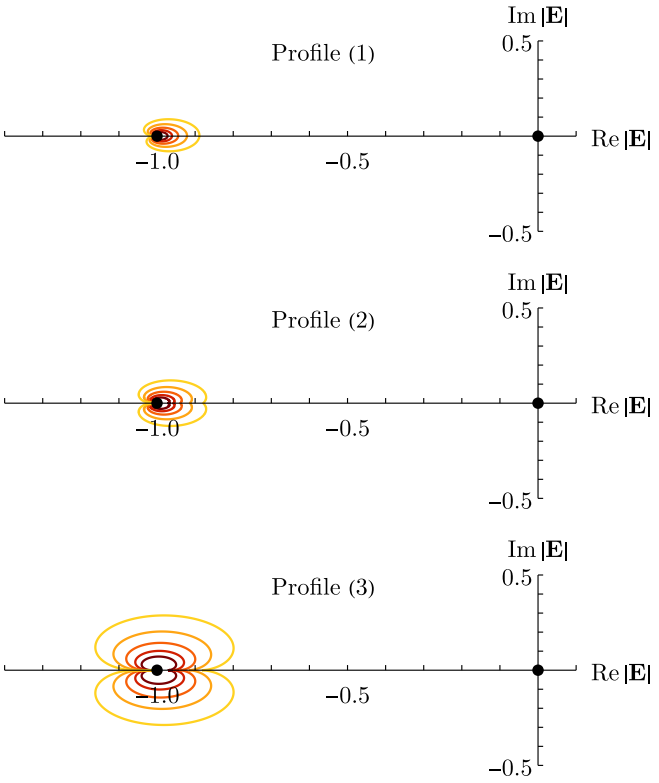

FIG. 4. Nyquist contours, $\omega_{\mathrm{R}} \mapsto |\mathbf{E}(\omega_{\mathrm{R}})|$, for $p_\theta = 1$ and the various frequency profiles from Eqs. (4), as one increases G (red to yellow) for the values presented in Table I.

In Fig. 4, we illustrate the Nyquist contours (see, e.g., Ref. [40]), $\omega_{\mathrm{R}} \mapsto |\mathbf{E}(\omega_{\mathrm{R}})|$, for the three frequency profiles, as one varies the coupling amplitude, G. Following Eq. (B5), the closer $\mathbf{E}(\omega)$ is from the identity-like matrix $\mathbf{\Gamma}$, the closer the dressed coupling coefficients U_k^{d} are from the bare ones U_k, i.e., the more negligible the collective effects. Phrased differently, the smaller G, the closer the contour from the

TABLE I. Integration parameters for the profiles from Eqs. (4).

All profiles	
G_{max}	$G_{\mathrm{crit}}/3$
G	$2^{-n/4} \times G_{\mathrm{max}}$ $(0 \leqslant n \leqslant 4)$
N	$\lfloor 2^{n/4} \times N_{\mathrm{min}} \rceil$ $(0 \leqslant n \leqslant 4)$
Profile	**(1)**
$G_{\mathrm{crit}}; N_{\mathrm{min}}$	1.85; 1024
Time step h	$(N/N_{\mathrm{min}})^{1/2}/50000$
Total time T_{max}	$10^2 \times (N/N_{\mathrm{min}})\,(G/G_{\mathrm{max}})^{-2}$
Profile	**(2)**
$G_{\mathrm{crit}}; N_{\mathrm{min}}$	8.95; 32
Timestep h	$(G/G_{\mathrm{max}})/3500$
Total time T_{max}	$2.3 \times 10^5 \times (N/N_{\mathrm{min}})^2\,(G/G_{\mathrm{max}})^{-4}$
Profile	**(3)**
$G_{\mathrm{crit}}; N_{\mathrm{min}}$	9.87; 32
Time step h	$(G/G_{\mathrm{max}})^2/1500$
Total time T_{max}	$9.3 \times 10^4 \times (N/N_{\mathrm{min}})^2\,(G/G_{\mathrm{max}})^{-6}$

point $\det \mathbf{\Gamma} = (-1, 0)$, i.e., the hotter are the systems. In practice, the ranges of G effectively simulated are detailed in Table I.

APPENDIX B: $1/N$ KINETIC EQUATIONS

Following the notations from Sec. III A, the inhomogeneous $1/N$ Landau equation generically reads [11]

$$\frac{\partial F(J)}{\partial t} = 2\pi\mu \frac{\partial}{\partial J}\Bigg[\sum_{k_1} k_1 \int \mathrm{d}J_1 \, |U_{k_1}(\mathbf{J})|^2 \times \delta_{\mathrm{D}}(\mathbf{k}\cdot\mathbf{\Omega})\, \mathbf{k}\cdot\frac{\partial}{\partial \mathbf{J}} F_2(\mathbf{J})\Bigg]. \tag{B1}$$

In this equation, the bare coupling coefficients, $U_k(J, J')$, are the Fourier transform with respect to the angles (θ, θ') of the interaction potential, $U(|\theta - \theta'|, \{J, J'\})$. They read

$$U(\mathbf{w}, \mathbf{w}') = \sum_{k=-\infty}^{+\infty} U_k(J, J')\, \mathrm{e}^{\mathrm{i}k(\theta-\theta')}, \tag{B2}$$

with

$$U_k(J, J') = \int \frac{\mathrm{d}\theta}{2\pi}\frac{\mathrm{d}\theta'}{2\pi} U(\mathbf{w}, \mathbf{w}')\, \mathrm{e}^{-\mathrm{i}k(\theta-\theta')}. \tag{B3}$$

Following Eqs. (A2) and (A5), the bare coupling coefficients can equivalently be rewritten using the basis elements to become

$$U_k(J, J') = -\sum_{p,q} \psi_k^{(p)}(J)\, \Gamma_{pq}\, \psi_k^{(q)*}(J'). \tag{B4}$$

For an interaction potential of typical amplitude G, one has $U_k \propto G$, so that the relaxation sourced by Eq. (B1) occurs on a timescale of order $T_{\mathrm{r}} \propto T_{\mathrm{d}} N/G^2$.

When accounting for collective effects, the $1/N$ Landau equation becomes the $1/N$ BL equation [9,10]. It is straightforwardly obtained from Eq. (B1) by replacing the bare coupling coefficients with their (frequency-dependent) dressed analogs $U_k^{\mathrm{d}}(J, J', \omega)$. Using the self-consistency relation from Eq. (F5) in [41], they read

$$U_k^{\mathrm{d}}(J, J', \omega) = -\sum_{p,q} \psi_k^{(p)}(J)\, E^{-1}_{pq}(\omega)\, \psi_k^{(q)*}(J'), \tag{B5}$$

with $\mathbf{E}$ the dielectric matrix from Eq. (A3). In practice, in the $1/N$ BL equation, the dressed coupling coefficients are evaluated at the resonant frequency $\omega = k\,\Omega(J)$. Accordingly, in Sec. III A, we shorten the notations and write $U_k^{\mathrm{d}}(J, J') = U_k^{\mathrm{d}}(J, J', k\,\Omega[J])$.

APPENDIX C: $1/N^2$ LANDAU EQUATION

We reproduce here the inhomogeneous $1/N^2$ Landau equation presented in Eq. (4) of Ref. [19]. Using the notations from Sec. III B, it reads

$$\frac{\partial F(J)}{\partial t} = 2\pi^3\mu^2 \frac{\partial}{\partial J}\Bigg[\sum_{k_1,k_2} (k_1+k_2)\, \mathcal{P}\int \mathrm{d}J_1 \mathrm{d}J_2 \, |\Lambda_{k_1k_2}(\mathbf{J})|^2 \times \delta_{\mathrm{D}}[\mathbf{k}\cdot\mathbf{\Omega}] \left(\mathbf{k}\cdot\frac{\partial}{\partial \mathbf{J}}\right) F_3(\mathbf{J})\Bigg]. \tag{C1}$$

In that expression, the sum over the resonance vectors (k_1, k_2) is restricted to those such that k_1, k_2, and $k_1 + k_2$ are all nonzeros. Equation (C1) also involves $\mathcal{P}$, the Cauchy principal value, acting on the integral over $\mathrm{d}J_1$, and we refer to Sec. C2 in Ref. [19] to prove the well-posedness of the associated high-order resonant denominator. Finally, the coupling coefficients, $\Lambda_{k_1k_2}(\mathbf{J})$, read (see Sec. B in Ref. [19])

$$\Lambda_{k_1k_2}(\mathbf{J}) = \frac{[\Omega(J) - \Omega(J_1)]\,\mathcal{U}^{(1)}_{k_1k_2}(\mathbf{J}) + k_2\,\mathcal{U}^{(2)}_{k_1k_2}(\mathbf{J})}{k_1(k_1+k_2)[\Omega(J) - \Omega(J_1)]^2}, \tag{C2}$$

with the coupling functions $\mathcal{U}^{(1,2)}$ defined in the same section. Equation (C1) conserves the total mass, energy, and momentum, and satisfies an H theorem [19]. Importantly, for an interaction potential of amplitude G, one has $\mathcal{U}^{(1,2)}_{k_1k_2}(\mathbf{J}) \propto G^2$. The relaxation sourced by Eq. (C1) occurs therefore on a timescale of order $T_{\mathrm{r}} \propto T_{\mathrm{d}} N^2/G^4$.

APPENDIX D: $1/N^3$ LANDAU EQUATION

Our goal in this Appendix is not to derive a detailed kinetic equation but rather to investigate the scaling with respect to N and G of the resulting evolution, when driven by $1/N^3$ effects in the hot limit. We follow Sec. A1 of Ref. [19] for the setup of the notations. The dynamics of an N-body system is exactly described by the BBGKY equations for the n-body DFs, $F_n = F_n(\mathbf{w}_1, \ldots, \mathbf{w}_n, t)$. They read

$$\frac{\partial F_n}{\partial t} + [F_n, H_n]_n + \int \mathrm{d}\mathbf{w}_{n+1} [F_{n+1}, \delta H_{n+1}]_{n+1} = 0, \tag{D1}$$

with the Poisson bracket

$$[f, h]_n = \sum_{i=1}^{n} \left(\frac{\partial f}{\partial \theta_i}\frac{\partial h}{\partial J_i} - \frac{\partial f}{\partial J_i}\frac{\partial h}{\partial \theta_i}\right). \tag{D2}$$

We also introduced the specific Hamiltonian

$$H_n = \sum_{i=1}^{n} U_{\mathrm{ext}}(\mathbf{w}_i) + \sum_{i<j}^{n} \mu\, U(\mathbf{w}_i, \mathbf{w}_j), \tag{D3}$$

as well as the specific interaction energy

$$\delta H_{n+1}(\mathbf{w}_1, \ldots, \mathbf{w}_{n+1}) = \sum_{i=1}^{n} U(\mathbf{w}_i, \mathbf{w}_{n+1}). \tag{D4}$$

Equation (D1) provides us with evolution equations for F_1 up to F_4.

To perform perturbative expansions with respect to the small parameter $1/N$, we rely on the cluster expansion [42]. For the sake of completeness, we explicitly reproduce here the associated expressions. For F_2, we introduce

$$F_2(1, 2) = F(1)\, F(2) + G_2(1, 2), \tag{D5}$$

using the shortened notation $1 = \mathbf{w}_1$. Similarly, the three-body DF, F_3, is expanded as

$$F_3(1, 2, 3) = F(1)\, F(2)\, F(3) + \sum_{a=1}^{3} F(a)\, G_2(\mathrm{rest}) + G_3(1, 2, 3), \tag{D6}$$

with rest $= (2, 3)$ when $a = 1$ and so forth. Similarly, we decompose F_4 as

$$\begin{aligned} F_4(1,2,3,4) = {} & F(1)F(2)F(3)F(4) \\ & + \sum_{a=1}^{3}\sum_{b=a+1}^{4} F(a)F(b)G_2(\text{rest}) \\ & + \sum_{a=1}^{4} F(a)G_3(\text{rest}) \\ & + \sum_{a=2}^{4} G_2(1,a)G_2(\text{rest}) \\ & + G_4(1,2,3,4). \end{aligned} \tag{D7}$$

Finally, the five-body DF, F_5, is decomposed as

$$\begin{aligned} F_5(1,2,3,4,5) = {} & F(1)F(2)F(3)F(4)F(5) \\ & + \sum_{a=1}^{3}\sum_{b=a+1}^{4}\sum_{c=b+1}^{5} F(a)F(b)F(c)G_2(\text{rest}) \\ & + \sum_{a=1}^{4}\sum_{b=a+1}^{5} F(a)F(b)G_3(\text{rest}) \\ & + \sum_{a=1}^{5}\sum_{b=a+2}^{a+4} F(a)G_2(a+1,b)G_2(\text{rest}) \\ & + \sum_{a=1}^{5} F(a)G_4(\text{rest}) \\ & + \sum_{a=1}^{4}\sum_{b=a+1}^{5} G_2(a,b)G_3(\text{rest}) \\ & + G_5(1,2,3,4,5), \end{aligned} \tag{D8}$$

with the periodic convention that $6 = 1$, $7 = 2 \ldots$. We note that these definitions ensure that all functions are symmetric with respect to the interchange of any two coordinates.

To check the sanity of Eqs. (D5)–(D8), one can compute the "norm" of the correlation functions, G_n, by integrating over all their variables. Recalling that (see, e.g., Sec. A1 in Ref. [26])

$$\int \mathrm{d}1 \ldots \mathrm{d}n\, F_n(1,\ldots,n) = \frac{N!}{(N-n)!}\mu^n, \tag{D9}$$

with the notation $\mathrm{d}1 = \mathrm{d}\mathbf{w}_1$, we find [45]

$$\int \mathrm{d}1\, F(1) = N\mu, \tag{D10a}$$

$$\int \mathrm{d}1\mathrm{d}2\, G_2(1,2) = -N\mu^2, \tag{D10b}$$

$$\int \mathrm{d}1\mathrm{d}2\mathrm{d}3\, G_3(1,2,3) = 2N\mu^3, \tag{D10c}$$

$$\int \mathrm{d}1\mathrm{d}2\mathrm{d}3\mathrm{d}4\, G_4(1,2,3,4) = -6N\mu^4, \tag{D10d}$$

$$\int \mathrm{d}1\mathrm{d}2\mathrm{d}3\mathrm{d}4\mathrm{d}5\, G_5(1,2,3,4,5) = 24N\mu^5. \tag{D10e}$$

Since $\mu \sim 1/N$, we have the expected scalings with respect to N, namely, $F \sim 1$ and $G_n \sim 1/N^{n-1}$.

The next step of the calculation is to inject the decompositions from Eqs. (D5)–(D8) into Eq. (D1) to obtain evolution equations for $\partial F/\partial t$ and $\partial G_n/\partial t$. These cumbersome manipulations are more easily performed using a computer algebra system, as explicitly detailed in [45].

To perform a truncation of the evolution equations at order $1/N^3$, we follow the same approach as in Ref. [19] and introduce the small parameter $\varepsilon = 1/N$. More precisely, we perform the replacements

$$\mu \to \mu\,\varepsilon, \tag{D11a}$$

$$G_2 \to \varepsilon G_2^{(1)} + \varepsilon^2 G_2^{(2)} + \varepsilon^3 G_2^{(3)}, \tag{D11b}$$

$$G_3 \to \varepsilon^2 G_3^{(2)} + \varepsilon^3 G_3^{(3)}, \tag{D11c}$$

$$G_4 \to \varepsilon^3 G_4^{(3)}, \tag{D11d}$$

$$G_5 \to \varepsilon^4 G_5^{(4)}. \tag{D11e}$$

Once these replacements are performed, we keep only terms up to order ε^3, and gather the terms order by order in ε. We are left with a series of evolution equations for the various correlation functions [45].

Assuming that $F(J,t)$ and $\mathrm{d}J$ are all of size 1 with respect to N and G, and introducing $U \propto G$ as the typical scale of the interaction potential, we are left with evolution equations scaling like

$$\frac{\partial F}{\partial t} = UG_2^{(1)} + UG_2^{(2)} + UG_2^{(3)}, \tag{D12a}$$

$$\frac{\partial G_2^{(1)}}{\partial t} + \Omega G_2^{(1)} = UG_2^{(1)} + \mu U, \tag{D12b}$$

$$\frac{\partial G_2^{(2)}}{\partial t} + \Omega G_2^{(2)} = UG_2^{(2)} + \mu UG_2^{(1)} + UG_3^{(2)}, \tag{D12c}$$

$$\frac{\partial G_2^{(3)}}{\partial t} + \Omega G_2^{(3)} = UG_2^{(3)} + \mu UG_2^{(2)} + UG_3^{(3)}, \tag{D12d}$$

$$\frac{\partial G_3^{(2)}}{\partial t} + \Omega G_3^{(2)} = UG_3^{(2)} + \mu UG_2^{(1)} + UG_2^{(1)}G_2^{(1)}, \tag{D12e}$$

$$\begin{aligned} \frac{\partial G_3^{(3)}}{\partial t} + \Omega G_3^{(3)} = {} & UG_3^{(3)} + \mu UG_2^{(2)} + UG_2^{(1)}G_2^{(2)} \\ & + \mu UG_3^{(2)} + UG_4^{(3)}, \end{aligned} \tag{D12f}$$

$$\begin{aligned} \frac{\partial G_4^{(3)}}{\partial t} + \Omega G_4^{(3)} = {} & UG_4^{(3)} + \mu UG_3^{(2)} + \mu UG_2^{(1)}G_2^{(1)} \\ & + UG_2^{(1)}G_3^{(2)}. \end{aligned} \tag{D12g}$$

Deriving a kinetic equation for $\partial F/\partial t$ amounts to solving, in sequence, this intricate hierarchy of coupled partial integro-differential equations.

Placing ourselves in the limit $U \ll 1$, i.e., neglecting collective effects, and assuming that the four-body correlation function, $G_4^{(3)}$, drives the dynamics, we find that the system's evolution is sourced by the sequence of resolutions [44]

$$G_2^{(1)} \to G_3^{(2)} \to G_4^{(3)} \to G_3^{(3)} \to G_2^{(3)} \to \partial F/\partial t. \tag{D13}$$

Following Eq. (D12), we then successively find the scalings [45]

$$G_2^{(1)} = \mu U, \tag{D14a}$$
$$G_3^{(2)} = \mu^2 U^2, \tag{D14b}$$
$$G_4^{(3)} = \mu^3 U^3, \tag{D14c}$$
$$G_3^{(3)} = \mu^3 U^4, \tag{D14d}$$
$$G_2^{(3)} = \mu^3 U^5, \tag{D14e}$$
$$\partial F/\partial t = \mu^3 U^6, \tag{D14f}$$

with $U \propto G$, the amplitude of the pairwise coupling. As a conclusion, in the hot limit, the relaxation driven by four-body correlations, i.e., by $G_4^{(3)}$, is associated with the (very) long relaxation time $T_{\rm r} \propto N^3/G^6$.

APPENDIX E: NUMERICAL SIMULATIONS

Our goal is to integrate a set of N particles governed by the Hamiltonian from Eq. (1), with the particular interaction potential from Eq. (2).

1. Equations of motion

Following Hamilton's equations, the motion obeys

$$\frac{\mathrm{d}\theta_i}{\mathrm{d}t} = \Omega_{\rm ext}(J_i) + G\sum_{j\neq i}^{N} \mu\, 2\,(J_i - J_j)\,\mathcal{B}_2[\theta_i - \theta_j], \tag{E1a}$$

$$\frac{\mathrm{d}J_i}{\mathrm{d}t} = -G\sum_{j\neq i}^{N} \mu\,(J_i - J_j)^2\,\mathcal{B}_2'[\theta_i - \theta_j], \tag{E1b}$$

with $\Omega_{\rm ext} = \mathrm{d}U_{\rm ext}/\mathrm{d}J$. Such a system has two invariants

$$E_{\rm tot} = \sum_{i=1}^{N} \mu\, U_{\rm ext}(J_i) + \sum_{i<j}^{N} \mu^2\, U(\mathbf{w}_i, \mathbf{w}_j), \tag{E2a}$$

$$J_{\rm tot} = \frac{1}{M_{\rm tot}} \sum_{i=1}^{N} \mu\, J_i. \tag{E2b}$$

Owing to the system's 2π periodicity, we always rewrap the angles θ_i within the interval $[0, 2\pi]$. In that case, the wrapping function from Eq. (3) reads

$$w_{2\pi}[\theta - \theta'] = |\theta - \theta'| = \begin{cases} \theta - \theta' & \text{if} \quad \theta' < \theta \\ \theta' - \theta & \text{if} \quad \theta < \theta', \end{cases} \tag{E3}$$

and similarly for its gradient

$$\frac{\mathrm{d}w_{2\pi}[\theta - \theta']}{\mathrm{d}\theta} = \mathrm{Sign}[\theta - \theta'] = \begin{cases} 1 & \text{if} \quad \theta' < \theta \\ -1 & \text{if} \quad \theta < \theta'. \end{cases} \tag{E4}$$

Two important remarks can be made from Eqs. (E3) and (E4). First, provided that the respective order of (θ, θ') is known, these two equations are separable with respect to both angles. This enables an accelerated evaluation of the forces, see Appendix E 2. Second, the pairwise force is discontinuous when two particles cross in angle space. As a consequence, high-order integration schemes can only be first-order accurate. These discontinuities are the main source of errors when integrating the system's dynamics, see Appendix E 3.

2. Multipole acceleration

A naive implementation of Eq. (E1) requires $O(N^2)$ evaluations. Fortunately, Eqs. (E3) and (E4) being quasiseparable, this evaluation can be accelerated using a multipole-like method.

Recalling that the angles θ_i are always rewrapped to the interval $[0, 2\pi]$, we first sort the particles according to θ_i, in $O(N \ln N)$ operations. Once explicitly expanded, Eqs. (E1) involve polynomials of second order in (θ_i, J_j). Defining the upper/lower moments as

$$P_{kk'}(\theta_i) = \sum_{\theta_j < \theta_i} \mu\, \theta_j^k\, J_j^{k'};$$

$$Q_{kk'}(\theta_i) = \sum_{\theta_j > \theta_i} \mu\, \theta_j^k\, J_j^{k'}, \tag{E5}$$

we can rewrite Eqs. (E1) as

$$\frac{\mathrm{d}\theta_i}{\mathrm{d}t} = \Omega_{\rm ext}(J_i) + \left.\frac{\mathrm{d}\theta_i}{\mathrm{d}t}\right|_P + \left.\frac{\mathrm{d}\theta_i}{\mathrm{d}t}\right|_Q, \tag{E6a}$$

$$\frac{\mathrm{d}J_i}{\mathrm{d}t} = \left.\frac{\mathrm{d}J_i}{\mathrm{d}t}\right|_P + \left.\frac{\mathrm{d}J_i}{\mathrm{d}t}\right|_Q. \tag{E6b}$$

In these expressions, the upper/lower contributions read

$$\begin{aligned} \frac{1}{G}\left.\frac{\mathrm{d}\theta_i}{\mathrm{d}t}\right|_P &= \left(\frac{1}{3} - \frac{1}{\pi}\theta_i + \frac{1}{2\pi^2}\theta_i^2\right)(J_i P_{00} - P_{01}) \\ &\quad + \frac{1}{\pi}\left(1 - \frac{1}{\pi}\theta_i\right)(J_i P_{10} - P_{11}) \\ &\quad + \frac{1}{2\pi^2}(J_i P_{20} - P_{21}), \end{aligned} \tag{E7a}$$

$$\begin{aligned} \frac{1}{G}\left.\frac{\mathrm{d}\theta_i}{\mathrm{d}t}\right|_Q &= \left(\frac{1}{3} + \frac{1}{\pi}\theta_i + \frac{1}{2\pi^2}\theta_i^2\right)(J_i Q_{00} - Q_{01}) \\ &\quad - \frac{1}{\pi}\left(1 + \frac{1}{\pi}\theta_i\right)(J_i Q_{10} - Q_{11}) \\ &\quad + \frac{1}{2\pi^2}(J_i Q_{20} - Q_{21}), \end{aligned} \tag{E7b}$$

as well as

$$\begin{aligned} \frac{1}{G}\left.\frac{\mathrm{d}J_i}{\mathrm{d}t}\right|_P &= \frac{1}{2\pi} J_i \left(1 - \frac{1}{\pi}\theta_i\right)(J_i P_{00} - 2P_{01}) \\ &\quad + \frac{1}{2\pi}\left(1 - \frac{1}{\pi}\theta_i\right) P_{02} \\ &\quad + \frac{1}{2\pi^2}\left(J_i^2 P_{10} - 2J_i P_{11} + P_{12}\right), \end{aligned} \tag{E8a}$$

$$\begin{aligned} \frac{1}{G}\left.\frac{\mathrm{d}J_i}{\mathrm{d}t}\right|_Q &= -\frac{1}{2\pi} J_i \left(1 + \frac{1}{\pi}\theta_i\right)(J_i Q_{00} - 2Q_{01}) \\ &\quad - \frac{1}{2\pi}\left(1 + \frac{1}{\pi}\theta_i\right) Q_{02} \\ &\quad + \frac{1}{2\pi^2}\left(J_i^2 Q_{10} - 2J_i Q_{11} + Q_{12}\right). \end{aligned} \tag{E8b}$$

To compute the rates of change, one scrolls through the angles-sorted particles in increasing order (respectively,

decreasing order) while accumulating the various $\{P_{kk'}\}$ [resp. $\{Q_{kk'}\}$]. This is performed in $O(N)$ operations.

3. Time integration

Because the interaction potential from Eq. (2) has discontinuous derivatives, it is ill-advised to use high-order integration schemes. In practice, we use the explicit midpoint rule with a fixed time step, h. To integrate $\dot{y} = f(y)$ with $y = \{\theta_i, J_i\}_i$, we compute the transformation $y(t = nh) = y_n \to y_{n+1}$ via

$$f_1 = f(y_n), \tag{E9a}$$
$$y_1 = y_n + \tfrac{1}{2} h f_1, \tag{E9b}$$
$$f_2 = f(y_1), \tag{E9c}$$
$$y_{n+1} = y_n + h f_2. \tag{E9d}$$

Because the force $f(y)$ is discontinuous, the method from Eq. (E9) is only first order. This therefore requires the use of very small time steps, h, as we now detail.

4. Integration errors

We are interested in (very) long-term simulations for different values of (N, G). We must therefore carefully pick our integration parameters to ensure an appropriate conservation of the systems' invariants.

We first consider the relative error in $J_{\rm tot}$, as defined in Eq. (E2b). Up to round-off errors, our computation of the rates of change in Appendix E 2 conserves $J_{\rm tot}$, i.e., $\sum_{i=1}^{N} \mu \dot{J}_i = 0$. The midpoint method from Eq. (E9) conserves linear invariants [see, e.g., Ref. [46]]. Therefore, the relative error in $J_{\rm tot}$ will grow from the (biased) accumulation at every time step of a round-off error of order $\epsilon_0 \simeq 10^{-16}$. The final relative error in $J_{\rm tot}$ is then expected to scale like

$$\epsilon_{J_{\rm tot}}^{\rm final} \propto \epsilon_0 \, T_{\rm max}/h, \tag{E10}$$

with $T_{\rm max}$ the total integration time.

Let us now consider the relative error in $E_{\rm tot}$, as defined in Eq. (E2a). For small enough time steps, errors will mainly accumulate when particles collide in θ space, i.e., when their angles cross, therefore experiencing the discontinuity from Eq. (E4).

Let us assume that particles 1 and 2 cross. At the time of crossing, the respective force between the two particles changes abruptly by a factor of order G/N [see Eq. (E4)]. Then, the force on the two particles remains incorrect for this amount for a duration of order h. During one such time step, the typical error introduced in the phase-space position of the two particles is then $\epsilon_{12} \propto Gh/N$. Since we are in the dynamically hot limit, i.e., $G \to 0$, the main source of error in Eq. (E2a) stems from the total kinetic energy. Hence, after one collision, the relative error introduced in $E_{\rm tot}$ is of order $\epsilon_{E_{\rm tot}} \propto \epsilon_{12}/N$. There are about $O(N^2)$ angle collisions per dynamical time (which we take to be unity). Assuming that errors accumulate in quadrature, we finally find that final relative error in $E_{\rm tot}$ scales like

$$\epsilon_{E_{\rm tot}} \propto Gh T_{\rm max}^{1/2}/N. \tag{E11}$$

In practice, ensuring a good enough conservation of $E_{\rm tot}$ is the main constraint to consider when setting up the simulations.

5. Simulation setups

For a given frequency profile, we need to ensure that our final errors in $E_{\rm tot}$ remain similar as one varies (N, G). For all the simulations, we always consider the same initial DF, namely,

$$F(J) \propto \mathrm{e}^{-J^4}, \tag{E12}$$

correctly normalized. This DF is picked because it is not the steady state of any of the external potentials from Eqs. (4). We appropriately tune the total integration time, $T_{\rm max}$, and the integration time step, h, as follows.

Integration times. To observe relaxation, we take $T_{\rm max} \propto T_{\rm r}$ [Eqs. (8)]. We therefore choose

$$(1) \quad T_{\rm max} \propto N/G^2, \tag{E13a}$$
$$(2) \quad T_{\rm max} \propto N^2/G^4, \tag{E13b}$$
$$(3) \quad T_{\rm max} \propto N^2/G^6. \tag{E13c}$$

Integration time steps. We fix h so the final relative error in $E_{\rm tot}$ [Eq. (E11)] is independent of (N, G). In practice, we find

$$(1) \quad h \propto N^{1/2}, \tag{E14a}$$
$$(2) \quad h \propto G, \tag{E14b}$$
$$(3) \quad h \propto G^2. \tag{E14c}$$

Computational cost. The difficulty of integrating for one time step scales like $O(N \ln N)$ (Appendix E 2). Hence, the difficulty of performing one full integration scales like $O(N T_{\rm max} \ln N/h)$. For the different frequency profiles, we find

$$(1) \quad \text{Diff} \propto N^{3/2} \ln N/G^2, \tag{E15a}$$
$$(2) \quad \text{Diff} \propto N^3 \ln N/G^5, \tag{E15b}$$
$$(3) \quad \text{Diff} \propto N^3 \ln N/G^8. \tag{E15c}$$

As expected, the integrations for profile (3) are the most challenging ones.

Following these guidelines, to obtain Fig. 2, we used the integration parameters from Table I. For every frequency profile and every value of (N, G), we perform a total of $N_{\rm real} = 10^3$ realizations. These are time-consuming simulations. Indeed, on a 128-core CPU, running 50 independent realizations for all 25 values of (N, G) required $\sim$3 hr (respectively, $\sim$140 hr; $\sim$150 hr) for profile (1) [respectively, (2); (3)].

In Fig. 5 (respectively, Fig. 6), we illustrate the time dependence of the relative errors in $E_{\rm tot}$ (respectively, $J_{\rm tot}$). As expected, simulations with different values of (N, G) show similar relative errors in $E_{\rm tot}$ at the end of their respective integrations.

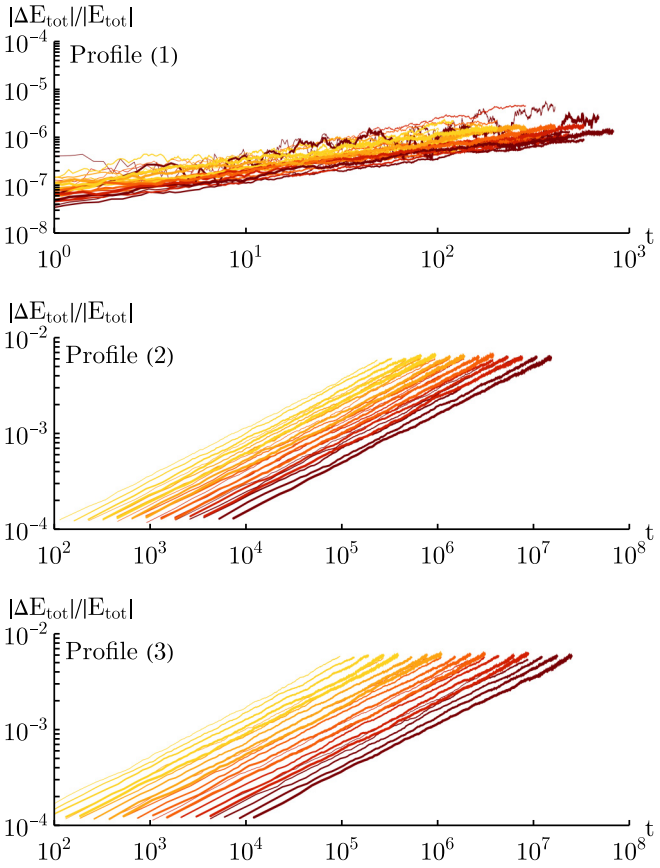

FIG. 5. Time evolution of the relative error in $E_{\rm tot}$ for the frequency profiles from Eqs. (4) (top to bottom panels) as one increases N (thin to thick) and increases G (red to yellow).

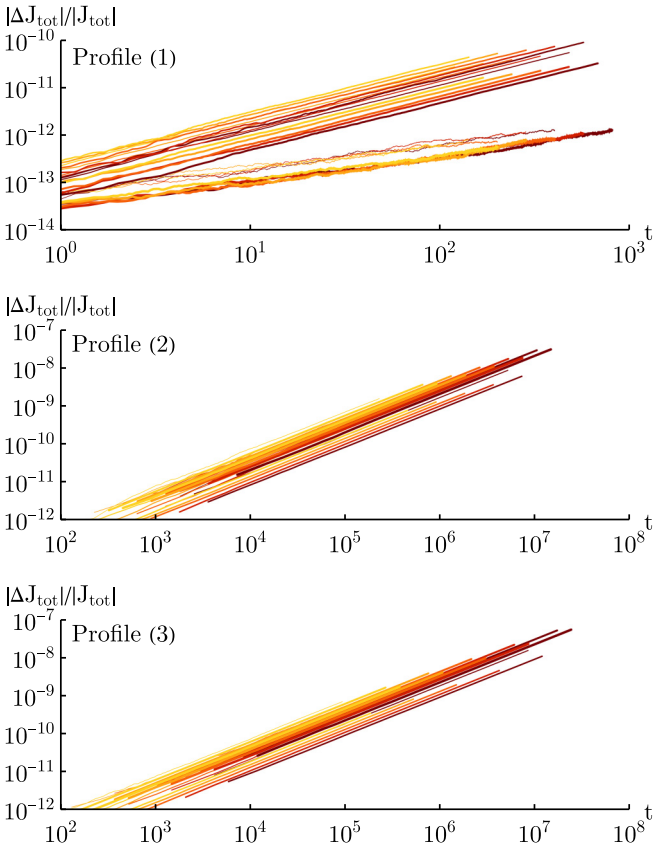

FIG. 6. Same as Fig. 5 but for $J_{\rm tot}$.

6. Measuring relaxation

We track relaxation via centered moments in action. Taking inspiration from [24,47], we consider

$$m_4(t) = \frac{1}{M_{\rm tot}} \sum_{i=1}^{N} \mu \, (J_i - J_{\rm tot})^4, \tag{E16}$$

where, up to integration errors, $J_{\rm tot}$ is conserved in every realization [Eq. (E2b)].

For a given frequency profile and a given value of (N, G), we have at our disposal a large set of realizations. Performing an ensemble-average over realizations, we are left with a time series of the form $t \mapsto \langle m_4(t) \rangle$, as illustrated in Fig. 7. During the first few dynamical times, the systems undergo a (slight) initial violent relaxation [1]. To prevent it from polluting our measurements, we only consider the signals for $t \geqslant 5$.

The crux of the measurement is then as follows. For a given time series, we perform a linear fit of the form

$$\langle m_4(t) \rangle \simeq \beta \, t + \text{cst.}, \tag{E17}$$

so that the slope $\beta = \beta(N, G)$ is expected to be proportional to $1/T_{\rm r}$. In Fig. 8, we illustrate the dependence of β as one varies (N, G). Then, having at our disposal a set of $\beta(N, G)$, we perform a linear fit of the form

$$\ln \beta(N, G) \simeq -\gamma_N \, \ln N + \gamma_G \, \ln G + \text{cst}. \tag{E18}$$

The coefficients (γ_N, γ_G) are the ones from Eq. (9).

In practice, it is important to estimate the uncertainties of this measurement. This is performed using bootstraps. A given bootstrap proceeds as follows. For every value of (N, G), we perform the ensemble average of $m_4(t)$ over a sample of $N_{\rm real}$ realizations drawn, with repetitions, from the $N_{\rm real}$ realizations available. Using the associated $\langle m_4(t) \rangle$, we perform the linear fit from Eq. (E17) from which we also estimate the variance of β. For every value of (N, G), we draw a value of $\beta(N, G)$ according to the associated Gaussian distribution. Finally, from this sample of $\beta(N, G)$, we perform the linear fit from Eq. (E18). Relying on the variance-covariance of (γ_N, γ_G), we can draw one value for (γ_N, γ_G), following the associated Gaussian distribution. This constitutes one bootstrap measurement. In practice, to obtain Fig. 2, we performed a total of 1280 bootstrap measurements.

Once these samples of $\boldsymbol{\gamma} = (\gamma_N, \gamma_G)$ are available, we estimate their associated probability distribution function, $P(\boldsymbol{\gamma})$, using MATHEMATICA's default `SmoothKernelDistribution`. Finally, a contour labeled $x\%$ in Fig. 2 corresponds to the level line $P(\boldsymbol{\gamma}) = p$, with p set by $Q(p)/Q(p=0) = x\%$ and $Q(p) = \int_{P(\boldsymbol{\gamma}) \geqslant p} \mathrm{d}\boldsymbol{\gamma} P(\boldsymbol{\gamma})$.

7. Bias in γ_G

In Fig. 2, the kinetic prediction for γ_G corresponds to the limit $G \to 0$, while the measurements are performed for finite values of G. This leads to a biased overestimation of γ_G, once again associated with leaks from collective effects. In

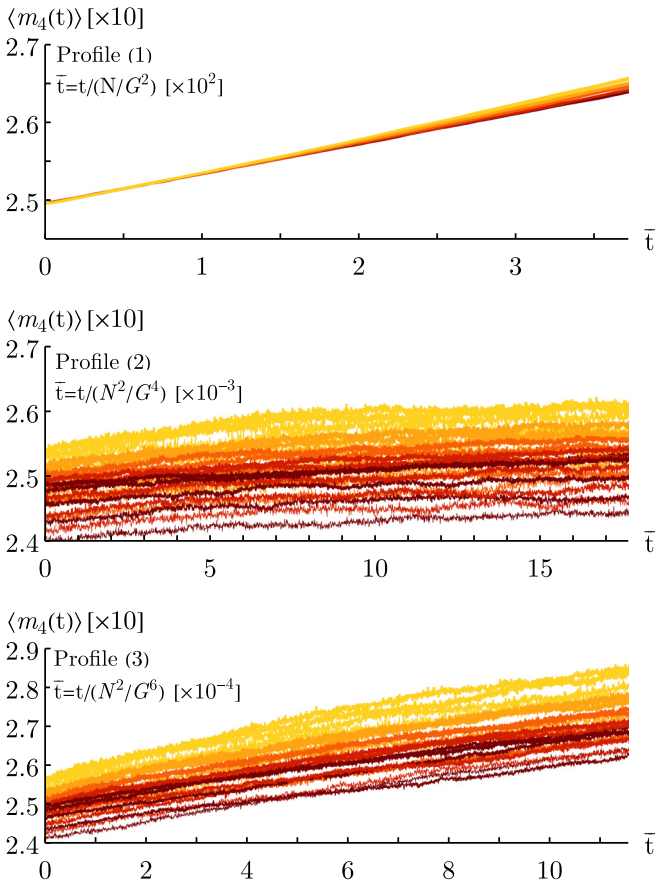

FIG. 7. Time evolution of the ensemble-averaged moment, $\langle m_4(t)\rangle$, for the different frequency profiles from Eqs. (4) (top to bottom panels) as one increases N (thin to thick) and increases G (red to yellow). The time axis has been rescaled following the expected relaxation time from Eqs. (8).

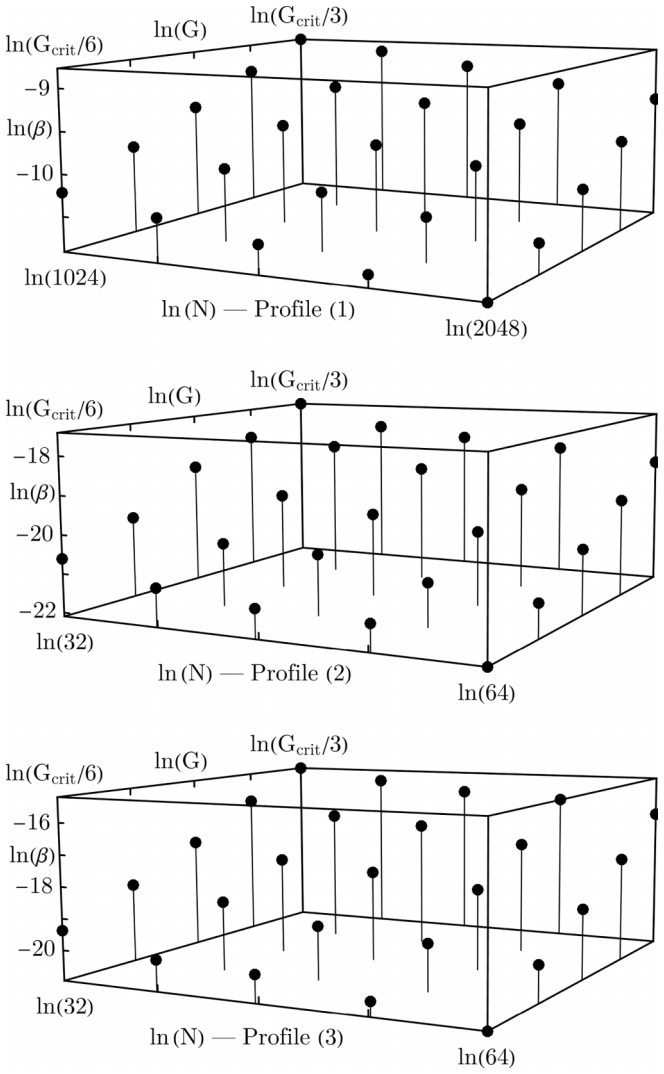

FIG. 8. Dependence of the slope $\ln\beta(N,G)$ for the different frequency profiles from Eqs. (4) (top to bottom panels) as a function of (N,G).

this section, we briefly estimate the maximum extent of that pollution.

For a fixed value of N, the scaling of the $1/N$ BL equation with respect to G is, roughly,

$$\frac{\partial F}{\partial t} \propto \left(\frac{G}{1-G/G_{\rm crit}}\right)^2. \tag{E19}$$

Here, we followed Eq. (B5) and wrote the dressed coupling coefficient as $U^{\rm d} \propto U/|\mathbf{E}| \propto G/(1-G/G_{\rm crit})$, and subsequently abruptly neglected the frequency dependence of the dielectric matrix, $\mathbf{E}(\omega)$.

Similarly, within the same limits and following Eq. (6), the $1/N^2$ BL equation is expected to scale with respect to G roughly like

$$\frac{\partial F}{\partial t} \propto \left(\frac{G}{1-G/G_{\rm crit}}\right)^4. \tag{E20}$$

When measuring numerically relaxation rates, we limited ourselves to the values $G/G_{\rm crit} = \{2^{-n/4}/3\}$ with $0 \leqslant n \leqslant 4$, as detailed in Table I. To estimate the maximum bias in γ_G associated with this particular choice, we can compute $\partial F/\partial t$ as given by Eqs. (E19) and (E20), and perform the linear fit $\ln(\partial F/\partial t) \simeq \widetilde{\gamma}_G \ln G + \text{cst}$. In that case, $\widetilde{\gamma}_G$ is then an estimate of the maximum value of γ_G that could stem from our use of finite values of G. In practice, for the $1/N$ (respectively, $1/N^2$) dynamics from Eq. (E19) [respectively, Eq. (E20)], we find $\widetilde{\gamma}_G \simeq 2.64$ (respectively, $\widetilde{\gamma}_G \simeq 5.28$). Fortunately, these values of $\widetilde{\gamma}_G$ are larger than the mean values obtained in Fig. 2. This strengthens our confidence in the sanity of the numerical measurements.

[1] D. Lynden-Bell, Mon. Not. R. Astron. Soc. **136**, 101 (1967).
[2] D. R. Nicholson, *Introduction to Plasma Theory* (Krieger, Malabar, FL, 1992).
[3] J. Binney and S. Tremaine, *Galactic Dynamics*, 2nd ed. (Princeton University Press, Princeton, NJ, 2008).
[4] F. Bouchet and A. Venaille, Phys. Rep. **515**, 227 (2012).

[5] A. Campa, T. Dauxois, D. Fanelli, and S. Ruffo, *Physics of Long-Range Interacting Systems* (Oxford University Press, Oxford, UK, 2014).

[6] J. Kormendy, in *Secular Evolution of Galaxies*, edited by J. Falcón-Barroso and J. H. Knapen (Cambridge University Press, Cambridge, UK, 2013), p. 1.

[7] T. Alexander, Astron. Astrophys. **55**, 17 (2017).

[8] D. Heggie and P. Hut, *The Gravitational Million-Body Problem* (Cambridge University Press, Cambridge, UK, 2003).

[9] J. Heyvaerts, Mon. Not. R. Astron. Soc. **407**, 355 (2010).

[10] P.-H. Chavanis, Physica A **391**, 3680 (2012).

[11] P.-H. Chavanis, Astron. Astrophys. **556**, A93 (2013).

[12] O. C. Eldridge and M. Feix, Phys. Fluids **6**, 398 (1963).

[13] D. H. E. Dubin, Phys. Plasmas **10**, 1338 (2003).

[14] F. Bouchet and T. Dauxois, Phys. Rev. E **72**, 045103(R) (2005).

[15] P.-H. Chavanis and M. Lemou, Eur. Phys. J. B **59**, 217 (2007).

[16] S. Gupta and D. Mukamel, J. Stat. Mech. (2011) P03015.

[17] J. Barré and S. Gupta, J. Stat. Mech. (2014) P02017.

[18] C. R. Lourenço and T. M. Rocha Filho, Phys. Rev. E **92**, 012117 (2015).

[19] J.-B. Fouvry, Phys. Rev. E **106**, 054123 (2022).

[20] This is not generically true for inhomogeneous systems whose action coordinate may have a semi-infinite support, as for the Hamiltonian mean field model [21] or point vortices (see e.g., Ref. [15]), or even a finite support, as for classical spins (see e.g., Refs. [16,17]).

[21] M. Antoni and S. Ruffo, Phys. Rev. E **52**, 2361 (1995).

[22] J. Jeans, Mon. Not. R. Astron. Soc. **76**, 70 (1915).

[23] C. Hamilton, Mon. Not. R. Astron. Soc. **501**, 3371 (2021).

[24] T. M. Rocha Filho, A. E. Santana, M. A. Amato, and A. Figueiredo, Phys. Rev. E **90**, 032133 (2014).

[25] J.-B. Fouvry, B. Bar-Or, and P.-H. Chavanis, Phys. Rev. E **100**, 052142 (2019).

[26] J.-B. Fouvry, P.-H. Chavanis, and C. Pichon, Phys. Rev. E **102**, 052110 (2020).

[27] P. Smereka, Physica D **124**, 104 (1998).

[28] J. Barré, A. Olivetti, and Y. Y. Yamaguchi, J. Phys. A Math. **44**, 405502 (2011).

[29] J. Barré and Y. Y Yamaguchi, J. Phys. A Math. **46**, 225501 (2013).

[30] E. Faou, R. Horsin, and F. Rousset, J. Dyn. Differ. Eqs. **33**, 1531 (2021).

[31] A. Campa, P.-H. Chavanis, A. Giansanti, and G. Morelli, Phys. Rev. E **78**, 040102(R) (2008).

[32] D. Das and S. Gupta, J. Stat. Mech. (2019) 084007.

[33] A. Rogister and C. Oberman, J. Plasma Phys. **2**, 33 (1968).

[34] C. Hamilton and T. Heinemann, Mon. Not. R. Astron. Soc. **525**, 4161 (2023).

[35] A. J. Kalnajs, Astrophys. J. **205**, 751 (1976).

[36] D. Dootson and J. Magorrian, arXiv:2205.15725.

[37] J.-B. Fouvry and S. Prunet, Mon. Not. R. Astron. Soc. **509**, 2443 (2022).

[38] M. Roule, J.-B. Fouvry, C. Pichon, and P.-H. Chavanis, Phys. Rev. E **106**, 044118 (2022).

[39] The interaction potential from Eq. (2) was devised in Ref. [19] from theoretical considerations. Unfortunately, as far as we know, this potential does not directly correspond to any physical system.

[40] P.-H. Chavanis and L. Delfini, Eur. Phys. J. B **69**, 389 (2009).

[41] J.-B. Fouvry and B. Bar-Or, Mon. Not. R. Astron. Soc. **481**, 4566 (2018).

[42] R. Balescu, *Statistical Dynamics: Matter out of Equilibrium* (Imperial College, London, 1997).

[43] Let us stress that, here, the coordinates, (θ, J), are not "instantaneous" angle-action coordinates self-consistently constructed from the current DF. Indeed, these coordinates are rather defined initially, once and for all, from the mean external potential.

[44] Unfortunately, the present argument is only heuristic, as we can only guess that some other sequence of resolutions, e.g., $G_2^{(1)} \to G_2^{(2)} \to G_2^{(3)} \to \partial F/\partial t$, will lead to vanishing contributions by symmetry. Though, the sequence from Eq. (D13) appears as the natural $1/N^3$ generalization of the $1/N^2$ sequence, $G_2^{(1)} \to G_3^{(2)} \to G_2^{(2)} \to \partial F/\partial t$, used to derive Eq. (C1) [19].

[45] See Supplemental Material at http://link.aps.org/supplemental/10.1103/PhysRevE.108.054108 for a heuristic derivation of the scaling of the $1/N^3$ Landau equation with respect to N, the number of particles.

[46] E. Hairer, C. Lubich, and G. Wanner, *Geometric Numerical Integration: Second Edition* (Springer, Berlin, 2006).

[47] M. Joyce and T. Worrakitpoonpon, J. Stat. Mech. (2010) P10012.